Spin- and valley-polarized Goos–Hänchen-like shift in ferromagnetic mass graphene junction with circularly polarized light

Mei-Rong Liu(刘美荣)[1], Zheng-Fang Liu(刘正方)[1,†], Ruo-Long Zhang(张若龙)[1], Xian-Bo Xiao(肖贤波)[2], and Qing-Ping Wu(伍清萍)[1,‡]

[1] *Department of Applied Physics, East China Jiaotong University, Nanchang* 330013, *China*
[2] *School of Computer Science, Jiangxi University of Chinese Medicine, Nanchang* 330004, *China*

(Received 20 May 2022; revised manuscript received 27 July 2022; accepted manuscript online 16 August 2022)

We investigate the band structure and Goos–Hänchen-like shift in ferromagnetic mass graphene junction modulated by the circularly polarized light. It is found that both spin and valley-related energy gaps can be opened by employing the circularly polarized light and the exchange field in mass graphene. The valley-polarized Goos–Hänchen-like shift can be identified in the presence of circularly polarized light, and the spin-polarized Goos–Hänchen-like shift can be realized with introduction of exchange field in mass graphene. Furthermore, the spin and valley polarization-related Goos–Hänchen-like shift can be achieved by combination of circularly polarized light and exchange field in mass graphene. It is hopeful that our work will be more conducive for future applications in graphene polarization transport devices.

Keywords: Goos–Hänchen-like shift, graphene, polarization

PACS: 73.23.–b, 72.25.–b **DOI:** 10.1088/1674-1056/ac89e2

1. Introduction

Graphene is a honeycomb crystal composed of a single layer of atomic structure.[1,2] It has ignited extensive interest because of its remarkable electronic properties[3,4] and unique electronic transmission characteristics.[5,6] More interestingly, by manipulating Dirac fermions in graphene with considering external fields, many optical-like electronic behaviors have been investigated and discovered,[7–10] such as Brewster angles,[7] Goos–Hänchen (GH) effect,[8] collimation,[10] and electronic lenses.[11]

The GH shift was first discovered at the total reflection interface, and it refers to the slight lateral displacement of the actual reflected beam relative to the geometrical optics predicted beam. Goos and Hänchen first confirmed such a shift experimentally,[12,13] and Artmann provided a theoretical explanation using the stationary phase method.[14] GH shift has been found to be tremendous and to have potential applications in many devices such as biosensors,[15] temperature sensors,[16] optical measurements,[17] and optical switches,[18] and has attracted abundant attentions in various materials and systems, involving microstructures and nanostructures,[19] quantum and plasma physics,[20] photonics crystals,[21] metamaterials,[22] and scientific research in graphene.[23,24] It has been demonstrated that the sublattice degree of freedom of massless Dirac fermions can affect the GH effect on the p–n interface in graphene.[8] Furthermore, the GH shifts have also been detected in bilayer graphene[25] and strained graphene.[7] In particular, it was extended to the partial reflection called Goos–Hänchen-like (GHL) shift. Similarly, GHL shift has also been applied to the studies in gaped graphene electrostatic barriers,[26] graphene double-barrier structures,[27] graphene superlattices,[28] and strained graphene.[29] Experimentally, GHL shift for magnetostatic spin waves has been observed.[30]

Recently, it has been shown that a valley-dependent energy gap[31] can be opened in the presence of both circularly polarized light and mass term.[32] The mass term can induce a sublattice symmetry breaking.[33] The configuration of ferromagnetic insulator (FI) deposited directly on top of graphene can induce exchange splitting, which is used to eliminate spin degeneracy.[34,35] Motivated by this, we propose and numerically demonstrate a novel configuration to obtain spin and valley polarization-related Goos–Hänchen-like shift in graphene junction. We consider a mass graphene sheet in the (x,y) plane. The FI stripe is deposited on top of the graphene sheet to realize an effective exchange field, and there is a circularly polarized light in the ferromagnetic graphene (barrier) regions. First, we investigate the band structure under different modulations and reveal the opening of the spin band gap and valley band gap. Then, we find that the valley-dependent GHL shift can be generated in the presence of circularly polarized light, the spin-dependent GHL shift can be bringed with the exchange field, and both the spin- and valley-dependent GHL shifts will emerge under the simultaneous modulation of the circularly polarized light and the exchange field in mass graphene. Finally, we confirm that there is an inseparable relationship between these exotic GHL shifts and the corresponding band gaps.

†Corresponding author. E-mail: lzhengfang@ecjtu.edu.cn
‡Corresponding author. E-mail: wuqingping78519@163.com

© 2023 Chinese Physical Society and IOP Publishing Ltd

2. Model and formalism

We take the existence mass of graphene sheet occupying the (x,y) plane, and apply the effective exchange field perpendicular to the plane in the FI stripe (barrier) regions (region Ⅱ), as sketched in Fig. 1. In addition, there is an off-resonant circularly polarized light field perpendicular to the barrier region.[36] The low-energy effective Hamiltonian is expressed as[32,37]

$$H = \hbar v_{\mathrm{F}}(k_x\tau_x - k_y\tau_y) - \tau_z(\eta\lambda_\Omega + \Delta) + sM. \tag{1}$$

Here, $v_{\mathrm{F}} \approx 10^6$ m/s is the Fermi velocity, $s = 1$ (-1) denotes up-spin (down-spin) orientations, and $\eta = 1$ (-1) for K (K') valleys, $\tau_{x,y,z}$ are the Pauli matrices in sublattice pseudo-spin space. Δ describes the mass term captured by a staggered potential term; λ_Ω is the effective energy induced by the off-resonant circularly polarized light;[38,39] and M is the effective exchange splitting obtained by the magnetic proximity effect of ferromagnetic insulators.[40]

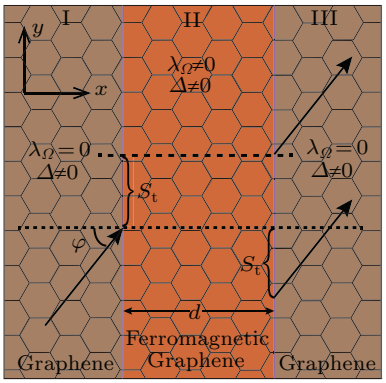


Fig. 1. Schematic diagram of the ferromagnetic mass graphene junction. There is the mass term all over the graphene sheet, which is shown by the Δ term. The FI stripe was deposited on top of the graphene layer in region Ⅱ, which was also modulated by the circularly polarized light (λ_Ω). The transport direction is along the x-axis.

Upon diagonalization of the Hamiltonian, we obtain the energy dispersion for both valleys as follows:

$$E_{\eta,s} = sM + \zeta\sqrt{(\hbar v_{\mathrm{F}}k)^2 + (\eta\lambda_\Omega + \Delta)^2}. \tag{2}$$

Here $\zeta = \pm$ stands for the conduction $(+)$ and valence $(-)$ bands. In the barrier region Ⅱ, the wave vector $q = \sqrt{(E - sM)^2 - (\eta\lambda_\Omega + \Delta)^2}/\hbar v_{\mathrm{F}}$. In the normal regions I and III, the wave vector $k = \sqrt{E^2 - \Delta^2}/\hbar v_{\mathrm{F}}$.

Due to the translational invariance in the y direction, k_y is conserved. The incident wave function is

$$\psi_{\mathrm{I}} = \begin{bmatrix} 1 \\ \frac{\alpha}{\beta}\mathrm{e}^{-\mathrm{i}\varphi} \end{bmatrix} \mathrm{e}^{\mathrm{i}(k_x x + k_y y)} + r \begin{bmatrix} 1 \\ -\frac{\alpha}{\beta}\mathrm{e}^{\mathrm{i}\varphi} \end{bmatrix} \mathrm{e}^{-\mathrm{i}(k_x x + k_y y)}. \tag{3}$$

The wave function in the transmitted region III can be expressed as

$$\psi_{\mathrm{III}} = t \begin{bmatrix} 1 \\ \frac{\alpha}{\beta}\mathrm{e}^{-\mathrm{i}\varphi} \end{bmatrix} \mathrm{e}^{\mathrm{i}(k_x x + k_y y)}, \tag{4}$$

with $\alpha = \sqrt{\frac{E-\Delta}{E}}$, $\beta = \sqrt{\frac{E+\Delta}{E}}$, $k_y = k\sin\varphi$, $k_x = k\cos\varphi$. Here φ is the incident angle; r and t are reflection and transmission probabilities, respectively.

The wave function in the region Ⅱ has the form

$$\psi_{\mathrm{II}} = \begin{bmatrix} 1 \\ \frac{\alpha_j}{\beta_j}\mathrm{e}^{-\mathrm{i}\theta} \end{bmatrix} \mathrm{e}^{\mathrm{i}(q_x x + k_y y)} + \begin{bmatrix} 1 \\ -\frac{\alpha_j}{\beta_j}\mathrm{e}^{\mathrm{i}\theta} \end{bmatrix} \mathrm{e}^{-\mathrm{i}(q_x x + k_y y)}, \tag{5}$$

where $\alpha_j = \sqrt{1 - \frac{\eta\lambda_\Omega + \Delta}{E - sM}}$ and $\beta_j = \sqrt{1 + \frac{\eta\lambda_\Omega + \Delta}{E - sM}}$.

According to the standard transfer matrix method,[41,42] the transmission probability

$$t_{\eta,s} = [\cos(q_x d) + \mathrm{i}\gamma_{\eta,s}\sin(q_x d)]^{-1}, \tag{6}$$

with

$$\gamma_{\eta,s} = \tan\theta\tan\varphi - \frac{k}{2aq_x\cos\varphi} - \frac{q}{2bk_x\cos\theta}, \tag{7}$$

where $a = E + \Delta$ and $b = E - sM - \eta\lambda_\Omega - \Delta$.

Thus, the phase of the transmission probability ϕ is obtained by

$$\phi_{\eta,s} = \arctan[-\gamma_{\eta,s}\tan(q_x d)]. \tag{8}$$

The stationary-phase approximation indicates that the GHL shift is equal to the negative gradient of transmission phase with respect to k_y. Therefore, the GHL shift is written as[43]

$$S_{\mathrm{t}}{}^{\eta,s} = -\frac{\partial\phi_{\eta,s}}{\partial k_y}. \tag{9}$$

3. Results and discussion

First, we investigate the band structure of the current elaborate graphene junction. Figure 2(a) presents that the mass term can only introduce a band gap due to the breaking of the inversion symmetry, while the spin and valley are both degenerate. However, by the introduction of circularly polarized light, the valley degeneracy can be lifted in the mass graphene, as shown in Fig. 2(b). At this point, based on Eq. (2), the energy band reads $E_{\eta,s} = \pm\sqrt{(\hbar v_{\mathrm{F}}k_x)^2 + (\eta\lambda_\Omega + \Delta)^2}$. One can find that only the spin states are degenerate, and the mass graphene with the help of the circularly polarized light can lift the valley degeneracy. Thus the valley-dependent gaps are produced, in which the electrons in the K and K' valleys are applied with different signs of circularly polarized light field. Therefore, valley-dependent GHL shift may be achieved with the circularly polarized light in mass graphene.

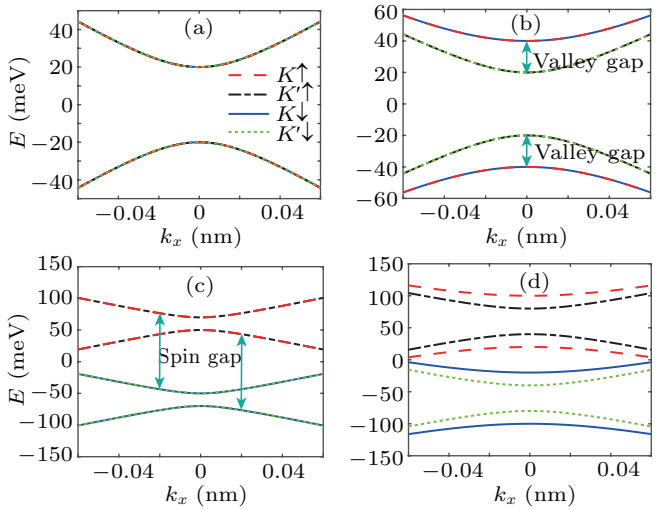


Fig. 2. Electronic band structures for spins and valleys as a function of k_x for $k_y = 0$, $d = 80$ nm: (a) $\lambda_\Omega = 0$ meV, $M = 0$ meV, and $\Delta = 20$ meV; (b) $\lambda_\Omega = 30$ meV, $M = 0$ meV, and $\Delta = 10$ meV; (c) $\lambda_\Omega = 0$ meV, $M = 60$ meV, and $\Delta = 10$ meV; (d) $\lambda_\Omega = 30$ meV, $M = 60$ meV, and $\Delta = 10$ meV.

Similarly, the energy band structures of the mass graphene with the exchange field are plotted in Fig. 2(c). As can be seen, the spin-degenerate bands are separated. Under the condition $k_y = 0$, the energy bands can be reduced to $E_{\eta,s} = sM \pm \sqrt{(\hbar v_F k_x)^2 + \Delta^2}$. Since the operator s acts on the exchange field M, the electron for spin up and spin down have different barriers, so the spin-dependent energy gaps appear. It can be speculated that we can realize the spin-dependent GHL shift in mass graphene by considering the exchange field.

Furthermore, we reveal the energy band structures in mass graphene with both the circularly polarized light and the exchange field (as seen in Fig. 2(d)). Indeed, both spin- and valley-dependent gaps appear in the band structures. In short, the physics of valley and spin-polarized energy bands is achievable under the modulation of polarized light and exchange field. Then, in the same configuration, it is possible to achieve the spin- and valley-dependent GHL shift.

Based on the above discussion, we calculate the transmission probability $T = |t|^2$ and GHL shifts S_t under different modulations, as shown in the upper and lower rows of Fig. 3, respectively. Here, S_t has been rescaled by λ_F, and λ_F is the Fermi wavelength of electrons, while d is rescaled by $q_x{}^{-1}$.

As the barrier width d increases, the trajectory of the transmission probability exhibits a perfect periodicity (see Figs. 3(a)–3(c)), while the corresponding GHL shift behaves an analogous periodic oscillations whose peaks continuously change (see Figs. 3(d)–3(f)). Interestingly, the electrons with the largest amplitudes of the periodic transmission probabilities will exhibit the largest and most eye-catching GHL shifts. Specifically, in Figs. 3(a) and 3(d), considering the mass graphene with the circularly polarized light, the transmission probability and GHL shifts of electrons from different valleys are significantly inconsistent. At the same time, the electrons in the K valley have the largest amplitude transmission probability (Fig. 3(a)), and the peaks of their GHL shifts are also larger than other electrons (Fig. 3(d)). Therefore, the existence of valley-polarized GHL shift can be affirmed in the mass graphene system with the circularly polarized light, which is consistent with the band structures in Fig. 2(b). This provides a good suggestion for designing valley filter.

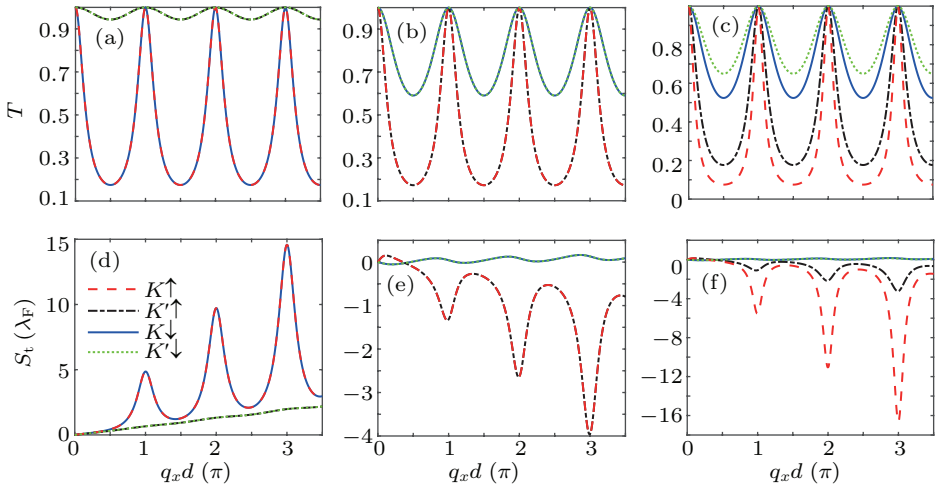


Fig. 3. The transmission probability T [(a)–(c)] and GHL shifts S_t [(d)–(f)] versus the barrier width d. The total angle $\varphi = 40°$ and the $\Delta = 10$ meV. The other parameters are [(a), (d)] $E = 60$ meV, $M = 0$ meV, and $\lambda_\Omega = 30$ meV; [(b), (e)] $E = 30$ meV, $M = 60$ meV, and $\lambda_\Omega = 0$ meV; [(c), (f)] $E = 60$ meV, $M = 30$ meV, and $\lambda_\Omega = 10$ meV.

In the presence of the exchange field in mass graphene, the transmission probability and GHL shifts are depicted in Figs. 3(b) and 3(e), respectively. We definitely reveal that the transmission probability and GHL shifts are spin-dependent. Although spin degeneracy is lifted and the spin gaps appear, there is no band gap between the conduction bands and the valence bands for spins. Moreover, the electron shift values for the spin up are all negative, which can be explained by the band structures shown in Fig. 2(c). For example, when $E = 40$ meV, there are the valence bands for $K\uparrow$ and $K'\uparrow$ and

the conduction bands for $K\downarrow$ and $K'\downarrow$ in the transmission channel. That is to say, there exists the Klein tunneling effect.[44] Therefore, the electrons for the spin up in Fig. 3(e) show the negative GHL shifts.

The transmission probability and GHL shifts in mass graphene with the circularly polarized light and the exchange field are demonstrated in Figs. 3(c) and 3(f). One can find that electrons with larger amplitudes of transmission probability correspond to larger GHL shifts, for example, the electrons for $K\uparrow$ and $K'\uparrow$. In Figs. 3(c) and 3(f), the transmission probability and the GHL shifts are both spin- and valley-dependent, which can be excellently explained by the band structures in Fig. 2(d). The occurrence of negative shifts is also related to the Klein tunneling effect. As a result, the GHL shifts of the transmitted electron beam from such a system are spin- and valley-polarized.

In order to further understand the effect of the circularly polarized light and the exchange field on GHL shifts in more detail, we further explore the transmission probability and the GHL shift as functions of the circularly polarized light and the exchange field in the following. With the increasing circularly polarized light λ_Ω, the transmission is forbidden, as shown in Fig. 4(a). Furthermore, it can be observed that the transmission forbidden regions of different valleys and spins are different. Physically, according to the threshold condition to turn on/off the propagating mode, i.e.,

$$(E_{\eta,s} - sM)^2 - (\eta\lambda_\Omega + \Delta)^2 \geq (E^2 - \Delta^2)\sin\varphi, \qquad (10)$$

we can derive that these critical points are $\lambda_\Omega = 20.4021$ meV for $K\uparrow$, $\lambda_\Omega = 60.4021$ meV for $K\downarrow$, $\lambda_\Omega = 127.0793$ meV for $K'\uparrow$ and $\lambda_\Omega = 167.0793$ meV for $K'\downarrow$, respectively. At positions slightly smaller than these critical points, the transmission probability turns into 1, which also corresponds to the presence of the S_t peaks. The S_t peaks of different valleys and spin are all different, the electrons for spin up present a negative GHL shifts, and down-spin electrons indicate a positive GHL shifts (as seen in Fig. 4(c)). Therefore, the GHL shifts can be tuned to spin- and valley-polarized with changing the intensity of circularly polarized light.

The effect of the exchange field on the GHL shifts has demonstrated in Fig. 4(d). For the different spin direction of an identical valley, the shifts of the opposite sign can be observed. For the K valley, for example, the red dotted line represents the negative shift for the spin-up electron, while the blue solid line denotes the positive shift for the spin-down electron. When the exchange field is small, the transmission is blocked. As the exchange field increases, the transmission block disappeared, and the transmission channel opened.

At the point where the transmission prohibition disappears, in the same way, according to Eq. (10), we can derive the critical point of the exchange field to be $M = 16.8406$ meV for $K'\downarrow$, $M = 54.2481$ meV for $K'\uparrow$, $M = 116.8406$ meV for $K\downarrow$, and $M = 154.2481$ meV for $K\uparrow$. In the vicinity of these critical values, the maximum transmission probability can be easily found, where the S_t peaks can be reliably attained. Therefore, it is possible to obtain the obvious GHL shift of the spin polarization and the valley polarization by adjusting the exchange field.

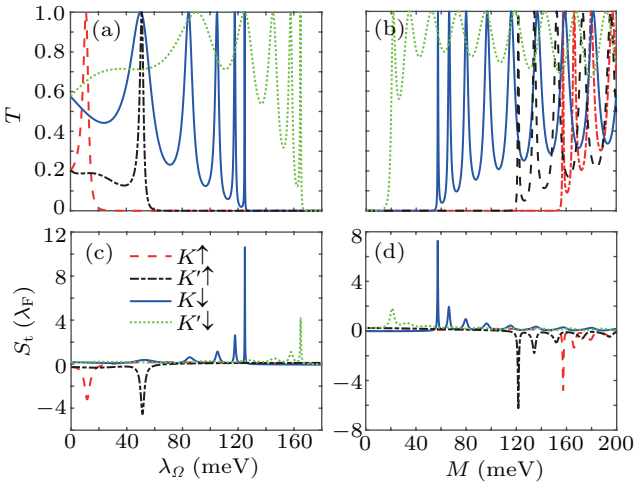


Fig. 4. The transmission probability T (a) and GHL shifts S_t (c) versus the circularly polarized light λ_Ω in mass graphene with $M = 100$ meV. The transmission probability T (b) and GHL shifts S_t (d) versus the exchange field M in mass graphene with $\lambda_\Omega = 80$ meV. The other parameters are the angle $\varphi = 40°$, $E = 50$ meV, $d = 80$ nm, and $\Delta = 20$ meV.

Combining with the above discussion, we can find that both the circularly polarized light and the exchange field have an influence on GHL shifts. We show the (λ_Ω, E) contour and (M, E) contour of the GHL shift in Fig. 5. In fact, the GHL shifts correspond to the energy band gap edge. Therefore, we reveal the band structure (as shown by the dotted line in Fig. 5). The band gap is between the two dashed lines. It is realized that the GHL shifts in the band gap are almost zero (see Fig. 5). For the energy bands of K valley in Fig. 5(a), the larger the circularly polarized light, the wider the energy band gap. However, for K' valley in Fig. 5(a), as the circularly polarized light increases, the band gap narrows from being wide, and finally becomes very wide. It can be found that at the edge of the band gap, the GHL shift value is larger, and the GHL shift peak is always manifested here. Noticeably, the band gaps for different valleys and spins are different. Accordingly, the GHL shifts also manifest disparate characteristics. For the exchange field as a function of the GHL shift (as seen in Fig. 5(b)), the energy dispersion has a linear relationship with the exchange field. With the increase of the exchange field, the S_t peaks of the up-spin electrons move in the direction of increasing energy. On the contrary, as the exchange field increases, the S_t peaks of the down-spin electrons move in the direction of decreasing energy. Due to the different energy band gaps, the GHL shifts for different valleys and spins are also different. Therefore, the GHL shifts are valley- and spin-polarized with the exchange field and the circularly polarized light modulated in the mass graphene.

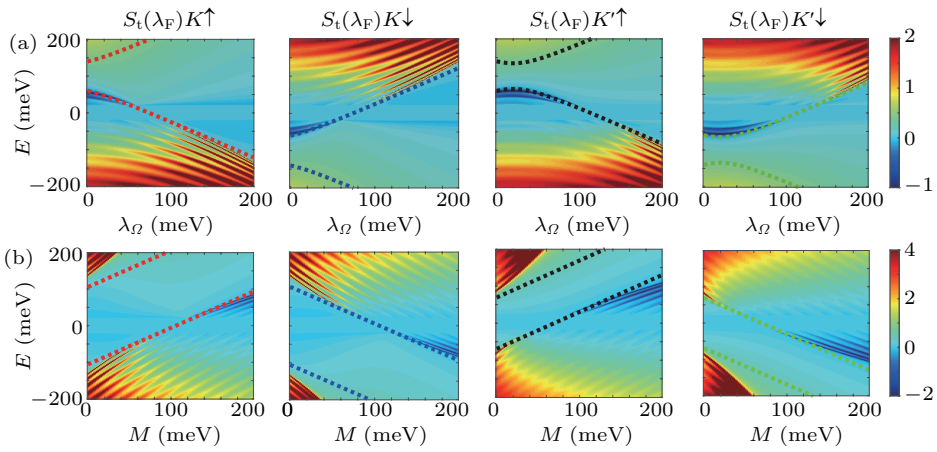


Fig. 5. The spin- and valley-dependent GHL shifts as a function of the incident energy and (a) the circularly polarized light, (b) the exchange field. The parameters are the same as those in Fig. 4. The dotted line represents the band structure under the corresponding parameters (in order to observe clearly, we set the spectrum range).

4. Conclusion

In summary, we have investigated the negative and positive GHL shifts for the electron beam transmitted through the ferromagnetic mass graphene junction with the circularly polarized light. When only considering the circularly polarized light in the mass graphene, the GHL shifts exhibit valley-related characteristics. While the mass graphene is only affected by the exchange field, spin-related GHL shifts occur. When both the circularly polarized light and the exchange field are applied to mass graphene, the GHL shift exhibits the characteristics of spin polarization and valley polarization. Furthermore, by controlling the strength of both the circularly polarized light and the exchange field, the system exhibits a positive or negative Goos–Hänchen-like shift, and the positions where these GHL shifts appear are closely related to the energy band structure. It is hopeful that our work will be useful for potential electronic device applications.

Acknowledgements

Project supported by the Natural Science Foundation of Jiangxi Province, China (Grant Nos. 20224BAB201025 and 20202BABL201018), and the National Natural Science Foundation of China (Grant Nos. 11864012, 11764013, and 12164021).

References

[1] Novoselov K S, Geim A K, Morozov S V, Jiang D, Zhang Y, Dubonos S V, Grigorieva I V and Firsov A A 2004 *Science* **306** 666
[2] Zhang Y, Tan Y W, Stormer H L and Kim P 2005 *Nature* **438** 201
[3] Beenakker, C 2008 *Rev. Mod. Phys.* **80** 1337
[4] Neto A C, Guinea F, Peres N M, Novoselov K S and Geim A K 2009 *Rev. Mod. Phys.* **81** 109
[5] Schwierz F 2010 *Nat. Nanotech.* **5** 487
[6] Xia F, Mueller T, Lin Y, Valdes-Garcia A and Avouris P 2009 *Nat. Nanotech.* **4** 839
[7] Wu Z, Zhai F, Peeters F, Xu H and Chang K 2011 *Phys. Rev. Lett.* **106** 176802
[8] Beenakker C W J, Sepkhanov R A, Akhmerov A R and Tworzydło J 2009 *Phys. Rev. Lett.* **102** 146804
[9] Darancet P, Olevano V and Mayou D 2009 *Phys. Rev. Lett.* **102** 136803
[10] Park C H, Son Y, Yang L, Cohen M L and Louie S G 2008 *Nano Lett.* **8** 2920
[11] Cheianov V V, Fal'ko V and Altshuler B L 2007 *Science* **315** 1252
[12] Goos F and Hänchen H 1947 *Ann. Phys.* **436** 333
[13] Goos F and Lindberg-Hänchen H 1949 *Ann. Phys.* **440** 251
[14] Artmann K 1948 *Ann. Phys.* **437** 87
[15] Guo Y, Singh N M, Das C M, Ouyang Q, Kang L, Li K, Coquet P and Yong K T 2020 *Plasmonics* **15** 1815
[16] Wang X P, Yin C, Sun J J, Li H G, Wang Y, Ran M W and Cao Z Q 2013 *Opt. Express* **21** 13380
[17] Yin X and Hesselink L 2006 *Appl. Phys. Lett.* **89** 261108
[18] Sakata T, Togo H and Shimokawa F 2000 *Appl. Phys. Lett.* **76** 2841
[19] Soni J, Mansha S, Gupta S D, Banerjee A and Ghosh N 2014 *Opt. Lett.* **39** 4100
[20] Lee S Y, Le Deunff J, Choi M and Ketzmerick R 2014 *Phys. Rev. A* **89** 022120
[21] Soboleva I V, Moskalenko V V and Fedyanin A A 2012 *Phys. Rev. Lett.* **108** 123901
[22] Grosche S, Ornigotti M and Szameit A 2015 *Opt. Express* **23** 30195
[23] Moradi A 2018 *Europhys. Lett.* **120** 67002
[24] Chen S, Mi C, Cai L, Liu M, Luo H and Wen S 2017 *Appl. Phys. Lett.* **110** 031105
[25] Cheng M 2012 *Eur. Phys. J. B* **85** 1
[26] Chen X, Tao J W and Ban Y 2011 *Eur. Phys. J. B* **79** 203
[27] Jellal A, Redouani I, Zahidi Y and Bahlouli H 2014 *Physica E* **58** 30
[28] Chen X, Zhao P L and Lu X J 2013 *Eur. Phys. J. B* **86** 1
[29] Cao Z Z, Cheng Y F and Li G Q 2011 *Physica B* **407** 4254
[30] Stigloher J, Taniguchi T, Körner H, Decker M, Moriyama T, Ono T and Back C H 2018 *Phys. Rev. Lett.* **121** 137201
[31] Wu Q P, Liu Z F, Chen A X, Xiao X B and Liu Z M 2014 *Appl. Phys. Lett.* **105** 252402
[32] Chang L L, Wu Q P, Li Y Z, Zhang R L, Liu M R, Li,W Y, Liu F F, Xiao X B and Liu Z F 2021 *Physica E* **130** 114681
[33] Sachs B, Wehling T O, Katsnelson M I and Lichtenstein A I 2011 *Phys. Rev. B* **84** 195414
[34] Haugen Hå, Huertas-Hernando D and Brataas A 2008 *Phys. Rev. B* **77** 115406
[35] Wu Q P, Liu Z F, Chen A X, Xiao X B and Miao G X 2017 *J. Appl. Phys.* **121** 053906
[36] Liu M R, Liu Z F, Zhang R L, Xiao X B and Wu Q P 2021 *Chin. Phys. B* **30** 107302
[37] Zhou X, Xu Y and Jin G 2015 *Phys. Rev. B* **92** 235436
[38] Xiao D, Liu G B, Feng W, Xu X and Yao Wang 2012 *Phys. Rev. Lett.* **108** 196802
[39] Yao W, Xiao D and Niu Q 2008 *Phys. Rev. B* **77** 235406
[40] Masir M R, Vasilopoulos P, Matulis A and Peeters F 2008 *Phys. Rev. B* **77** 235443
[41] Wang L G and Zhu S Y 2010 *Phys. Rev. B* **81** 205444
[42] Bercioux D and De M A 2010 *Phys. Rev. B* **81** 165410
[43] Mekkaoui M, Jellal A and Bahlouli H 2019 *Physica E* **111** 218
[44] Ghadiri H and Saffarzadeh A 2017 *J. Phys.: Condens. Matter* **29** 115303